

Assessing forest dynamic in Talassemtane National Park: A 34-year land cover change analysis using Google Earth Engine

Abdelazziz Chemchaoui^{1*}, Hassana Ismaili Alaoui¹, Souad Ghazi¹,
Hassan Boukita¹, Najiba Brhadda¹, Rabea Ziri¹

¹ Plant, Animal and Agro-Industry Production Laboratory, Faculty of Sciences, Ibn Tofail University, University Campus, Kenitra, 14000, Rabat Salé Kenitra, Morocco

* Corresponding author's e-mail: abdelaziz.chemvhaoui@uit.ac.ma

ABSTRACT

Land cover change detection offers multiple opportunities to spatial management specialists. Monitoring spatio-temporal dynamic is undoubtedly one of these key tasks. This study aims to monitor the forest dynamic of Talassemtane National Park over 34 years using merged composite cloud-masking Landsat images and Google Earth Engine a Google cloud product. This product provides a vast amount of geospatial data and algorithms to query, analyze, and visualize the data using simple script. The park's forests, which covered 43.600 hectares in 1990 (67% of the park), have lost more than 18% of their cover during this period, at an annual rate of 240 hectares. The largest reduction occurred between 1995 and 2000, with a significant loss of 4.411 hectares. The study results will be available to park managers to help them target interventions to conserve and develop the park's forests.

Keywords: land cover, change detection, forest loss, Talassemtane, Google Earth Engine.

INTRODUCTION

Forests worldwide, covering 3.97 billion hectares, or 30.8% of the world's land surface, are facing deforestation (FAO, 2022). Deforestation is defined as the conversion of forest to other land uses, regardless of the causes of conversion. Globally, deforestation affected 11 million hectares between 2000 and 2010, and 7.8 million hectares between 2010 and 2020 (FAO, 2022). Agricultural activities account for nearly 90% of these losses, with 50% attributed to cropland expansion and 38.5% to pasture (FAO, 2022). Deforestation is not the only cause of forest loss. Globally, only 27% of forest loss was associated with deforestation; the remainder was associated with forestry, shifting agriculture, forest fires, and urbanization (Curtis et al., 2018). In Morocco, the State forest domain covers 9,631.896 hectares, or 13.5% of the national coverage, including more than 3 million hectares of Alfa, (l'Agence Nationale des Eaux et Forêts Maroc, 2025). These areas are subject to an estimated degradation of 17,000 hectares per year

(Département des Eaux et Forêts Maroc, 2019). Other studies indicate losses of up to 30,000 hectares per year (Benbrahim et al., 2004). The causes of this degradation are of human origin (intense pressure on forests), natural (persistent drought), and management-related (dominance of a repressive approach) (Benzyane, 2007). In the northern region of Morocco, known for its biodiversity, drought, forest fires, soil erosion and population growth are the main causes of the disappearance of forests and agro-sylvopastoral lands between 1984 and 2014 (Chebli et al., 2018). In the Talassemtane National Park (TNP), a protected area in northern Morocco, forest fires and deforestation linked to cannabis cultivation are the main factors contributing to deforestation (Castro et al., 2022). This deforestation leads to a loss of biodiversity and threatens the last endemic species such as the Moroccan fir (*Abies maroccana Trabut*) and the black pine (*Pinus nigra*).

In recent developments in the Landsat Land Cover Classification Method, researchers around the world proposed a variety of methodologies

to assess, model, and predict deforestation. Land use land cover (LULC) analysis is the most used (García-álvarez et al., 2022). Land cover is described as the biological and physical covering of the earth's surface, but land use is defined as a region's present and planned functional dimensions or socioeconomic purposes are used to describe it. Researchers worldwide studied LULC analysis (García-álvarez et al., 2022). The use of LULC in several fields is well-established. LULC is used to assess vegetation structure and dynamics (El Haj et al., 2023; Nguyen et al., 2023), quantify soil erosion and map landslide susceptibility (Achariki et al., 2022; Alaoui et al., 2024; Aouragh et al., 2023; Bammou et al., 2024; Essmairi et al., 2023), map and model dynamic urban growth (Araya & Cabral, 2010; Benchelha et al., 2022; Farah et al., 2021; Hegazy & Kaloop, 2015), monitor and model desertification (El Haj et al., 2023; Moumane et al., 2022; Muteya et al., 2023), identify deforestation (Boubekraoui et al., 2023; Muteya et al., 2023), quantify forest loss and gain (Hansen et al., 2013; Kaur et al., 2023), map and update species distribution (Ghazi et al., 2024). Analyze changes in carbon stocks (Ismaili Alaoui et al., 2023; Rachid et al., 2024; Raqeeb et al., 2024), evaluate the impact of climate change on natural resources (M'Barek et al., 2024). In addition, LULC data provides important information by using change detection techniques (Lu et al., 2004). LULC changes are used to assess the spatiotemporal characteristics of LULC changes in China during 2010–2015 (Jia et al., 2018). The evolution of LULC, used to compare land use and land cover across different periods, can offer valuable insights into LULC dynamics (Bensaid, 2025; García-álvarez et al., 2022). Zeng et al. (2018) studied land surface temperature (LST) changes using Hansen's global forest change to assess the expansion of highland cropland and forest loss in Southeast Asia in the 21st century (Zeng et al., 2018). Studying LULC changes is essential to address global climate change and sustainable development (Chang et al., 2018), as LULC changes are both the cause and the consequence of climate change (Foody, 2010). Wang et al. (2023) conducted an analysis of land use and land cover (LULC) changes and their driving forces in a typical subtropical region of South Africa (Wang et al., 2023). Seyam et al. (2023) studied the trends in land use and land cover changes in a rapidly developing industrial region of Bangladesh (Seyam et al., 2023).

Moreover, the evolution of LULC and its factors enables specialists to predict the evolution of LULC in the future (García-álvarez et al., 2022; Muhammad et al., 2022; Yangouliba et al., 2022). The study of past and future changes in LULC is crucial for natural resource management, particularly for lake catchment management (Zhao et al., 2012), provides valuable information on the rate and extent of deforestation and its drivers (He et al., 2022), assessing island ecosystems and reforestation efforts (Lin et al., 2020), simulating urban growth (Abuelaish & Olmedo, 2016), assessing and simulating streamflow in watersheds (Eshetie et al., 2023), and predicting prompt urban growth (Vinayak et al., 2021; Wang et al., 2021). With the emergence of new AI-based classification techniques (Alshari & Gawali, 2021; Weng et al., 2024), the free availability of an archive of high-resolution satellite images (Tamiminia et al., 2020), and the development of cloud computing (Amani et al., 2020), the production of LULCs has grown exponentially. Google Earth Engine (GEE) is a cloud computing platform for global geospatial analysis using Google's cloud infrastructure. Continuously evolving, GEE enables users to visualize, analyze, and process multi-petabyte geospatial datasets from various providers (Gorelick et al., 2017). Its ability to rapidly process satellite imagery and run algorithms through Google's infrastructure makes it particularly well-suited for large-scale geographic data analysis (Tamiminia et al., 2020). GEE offers an application programming interface (API) that supports JavaScript and Python, allowing users to develop custom scripts to address big data processing challenges (Curtis et al., 2018; Tamiminia et al., 2020). The platform is widely used in fields such as agriculture, climate change, and land use, and its application to natural disaster management, especially flood monitoring, significantly improves the performance of algorithms (Amani et al., 2020; Ghosh et al., 2022; Pérez-cutillas et al., 2023). The growing use of GEE in producing scientific publications on the monitoring, modeling, and predicting changes in LULC is demonstrated by the impressive number of publications in this field (Tamiminia et al., 2020). Although access to GEE is free, it requires registration via a personal email account.

Consequently, this study aims to assess forest dynamics over 34 years in Talassemthane National Park (TNP). We used change detection techniques through GEE to assess the tree cover dynamic over this period.

MATERIALS AND METHODS

Study area

TNP is situated in the Western Rif Mountains of Morocco (Figure 1). This region is widely recognized for its ecological diversity, attributed to its unique morphology and favorable climatic conditions. However, it also faces significant environmental challenges, including a high rate of deforestation (Boubekraoui et al., 2024; Boubekraoui et al., 2024). Created in 2004, the TNP covers an area of 64,000 hectares. The park is particularly notable for hosting endemic species, such as the Moroccan fir (*Abies marocana*, *Pinaceae*) (Ben-Said, 2022; Lamrhari et al., 2020). The park's fir ecosystem has significant floristic diversity, with approximately 60 plant species identified (Aafi, 2000). In addition, the mixed forest of Moroccan fir and Atlas cedar is considered a unique ecosystem in the world (Ben-Said et al., 2022). Geologically, the park is located on a wide limestone ridge and its geomorphology presents the highest peaks in the park, with altitudes reaching up to 2,159 meters at Jbel Lakraa. From a bioclimatic point of view, the climate of the park varies from humid to perhumid due to its large area (Ben-Said et al., 2024). According to a soil map produced by Alaoui et al. (2021), the dominant soil types in the TNP are Cambisol, Rendzic Leptosol, Luvisol, Arenosol, and Regosol (Alaoui et al., 2021). With 105 people per km² in Chefchaouen and 316 people per km² in Tetouan, the TNP region has one of Morocco's highest population densities (Haut-Commissariat au Plan du Maroc, 2024).

Images composites

The datasets utilized in this study are images composites generated using the latest cloud masking approach as described by Hermosilla et al. (2024) (Hermosilla et al., 2024). Using JavaScript in GEE, we created images composites for the years 1990, 1995, 2000, 2005, 2010, 2015, 2020, and 2024 (Figure 2).

For 1990 and 1995, the dataset used was USGS Landsat 5 Level 2, Collection 2, Tier 1. The dataset includes 33 and 29 scenes, respectively, with six spectral bands, derived indices, Digital Surface Model (DSM), and slope data. For 2000, 2005, and 2010 two datasets were utilized: USGS Landsat 5 Level 2, Collection 2, Tier 1 and USGS Landsat 7 Level 2, Collection 2, Tier 1. For 2015, two datasets were used: USGS Landsat 7 Level 2, Collection 2, Tier 1 comprising 31 scenes, and USGS Landsat 8 Level 2, Collection 2, Tier 1 comprising 33 scenes (Table 1).

Finally, for 2024, the following datasets were utilized: USGS Landsat 8 Level 2, Collection 2, Tier 1. The image composite consists of 31 scenes with six spectral bands, derived indices, a digital surface model (DSM), and slope data. USGS Landsat 9 Level 2, Collection 2, Tier 1 consisting of 29 scenes. Four popular vegetation indices were used in this study to enhance classification accuracy and image interpretation (Bannari et al., 1995; Lloyd, 1990; Oldeland et al., 2010; Ouchra et al., 2023; Ustuner et al., 2014; Zhang et al., 2021), namely the normalized difference vegetation index (NDVI), the normalized difference built-up index (NDBI),

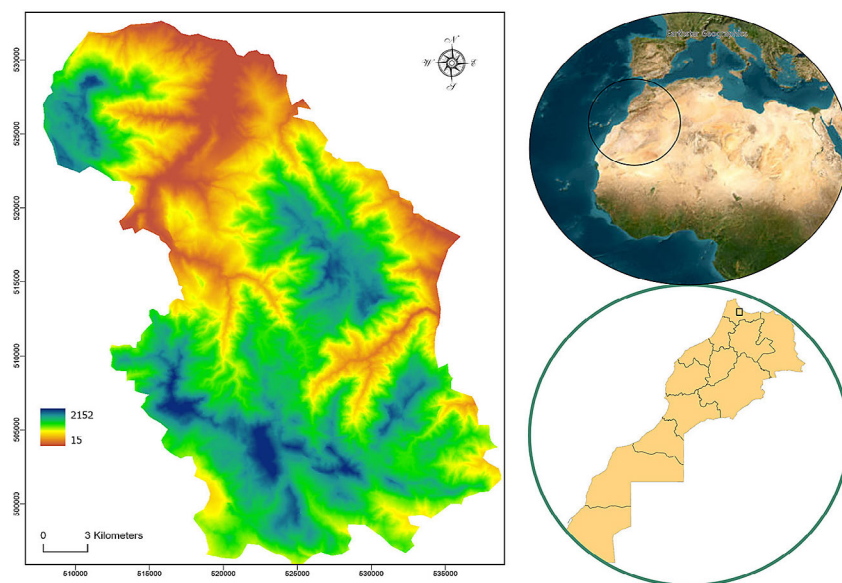


Figure 1. Geographic location of the study area

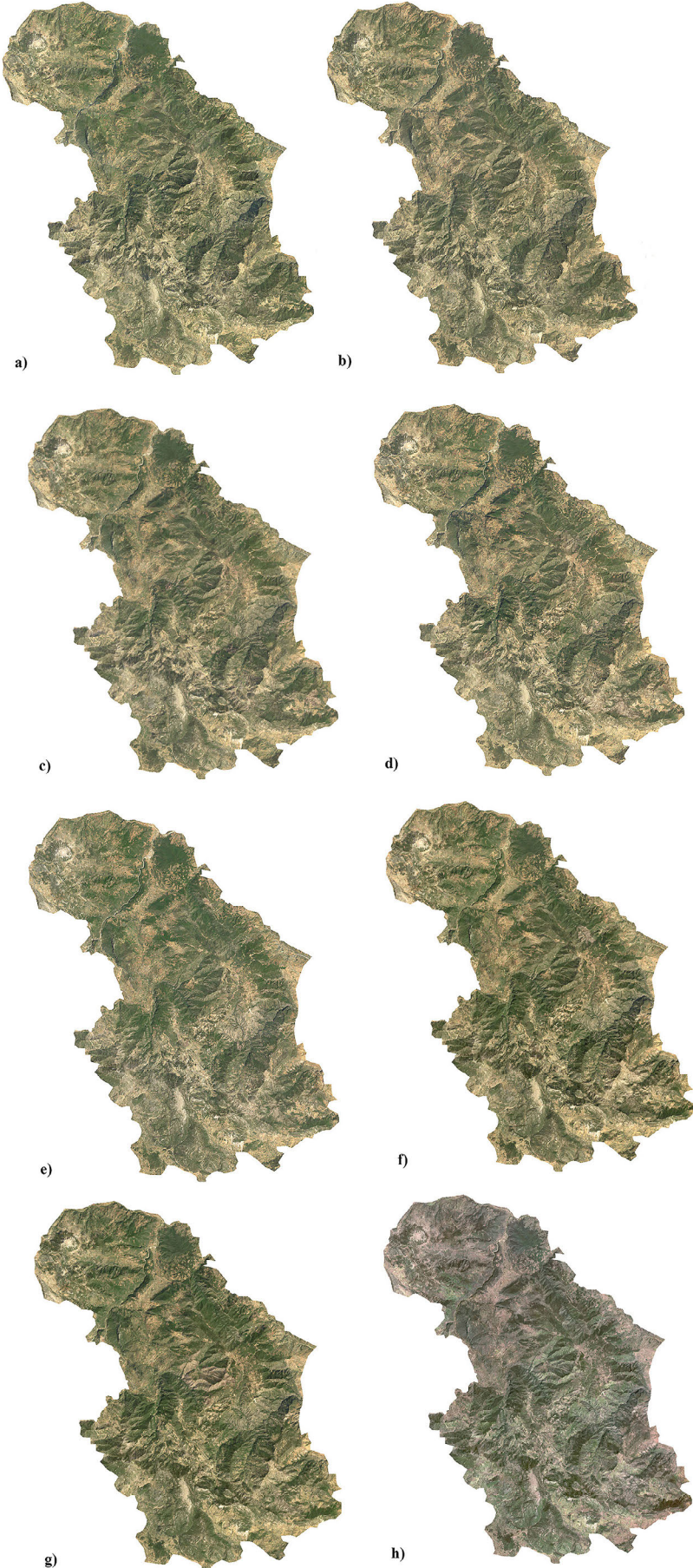


Figure 2. Yearly images collections (a) 1990, (b) 1995, (c) 2000, (d) 2005, (e) 2010, (f),2015, (g) 2020, (h) 2024

Table 1. Datasets used to produce Image collection for each year

Year	Datasets	features	Image collection
1990	USGS Landsat 5 Level 2, Collection 2, Tier 1	33	6 Bands + Indices + DSM+ Slope
1995	USGS Landsat 5 Level 2, Collection 2, Tier 1	29	6 Bands + Indices + DSM+ Slope
2000	USGS Landsat 5 Level 2, Collection 2, Tier 1	17	6 Bands + Indices + DSM+ Slope
	USGS Landsat 7 Level 2, Collection 2, Tier 1	36	
2005	USGS Landsat 5 Level 2, Collection 2, Tier 1	19	6 Bands + Indices + DSM+ Slope
	USGS Landsat 7 Level 2, Collection 2, Tier 1	17	
2010	USGS Landsat 5 Level 2, Collection 2, Tier 1	16	6 Bands + Indices + DSM+ Slope
	USGS Landsat 7 Level 2, Collection 2, Tier 1	16	
2015	USGS Landsat 7 Level 2, Collection 2, Tier 1	31	6 Bands + Indices + DSM+ Slope
	USGS Landsat 8 Level 2, Collection 2, Tier 1	33	
2020	USGS Landsat 7 Level 2, Collection 2, Tier 1	45	6 Bands + Indices + DSM+ Slope
	USGS Landsat 8 Level 2, Collection 2, Tier 1	37	
2024	USGS Landsat 8 Level 2, Collection 2, Tier 1	31	6 Bands + Indices + DSM+ Slope
	USGS Landsat 9 Level 2, Collection 2, Tier 1	29	

the modified normalized difference water index (NDWI), and the bare soil index (BSI) (Table 2).

Topographic variables were also incorporated into the classification process to improve accuracy (Tadono et al., 2014; H. Wang et al., 2020; Wulder et al., 2004). These variables included elevation and slope derived from digital elevation models (DEMs) (Table 3). The flow chart methodology of the study is presented in Figure 3.

Image classification

For image classification, we used machine learning algorithms running in GEE. GEE offer several machine learning classifiers in the ee.Classifier package. In our study, we used the ee.Classifier.smileRandomForest a popular supervised classification method based on the random forest (RF) algorithm. RF is a group learning method that uses multiple

decision trees to improve classification accuracy (Aziz et al., 2024; Lawer, 2024; Ouchra et al., 2024; Talukdar et al., 2020). In this study, we adopted only two classes: forest and noforest. The adoption of these two classes comes from the fact that the study concerns the evolution of the forest cover.

Accuracy assessment and hyper-parameter tuning

The choice of training samples is the first step in an accuracy assessment, followed by the collection of data from LULC map (classified data), the collection of reference data from either the visual interpretation of satellite imagery or data collected on-site (reference data), finally the analysis and interpretation of the findings (Congalton & Green, 2008). but in most research, the error matrix, overall accuracy, user accuracy, producer accuracy, and Kappa coefficient are among the statistical tools that are typically used (Chang et al., 2018; García-álvarez et al., 2022; Janssen & van der Wel, 1994). In addition, we used JavaScript through GEE to analyze and visualize the importance of variables in the trained classifier. Also, we use single parameter tuning to generate a chart of validation accuracy versus the number of trees.

Table 2. Indices used in the study

Indice	Formula
ndvi	$(nir-red)/(nir+red)$
ndbi	$(swir-nir)/(swir+nir)$
mndwi	$(green-swir)/(swir+nir)$
bsi	$((swir1+ red) - (nir + blue)) / ((swir1 + red) + (nir + blue))$

Table 3. Topographic variables

Variable	Source
Elevation	ALOS DSM: Global 30m v3.2
Slope	ALOS DSM: Global 30m v3.2

RESULTS

Classification

The results of the classification is presented in Table 4. Adopting two classes: forest and no forest

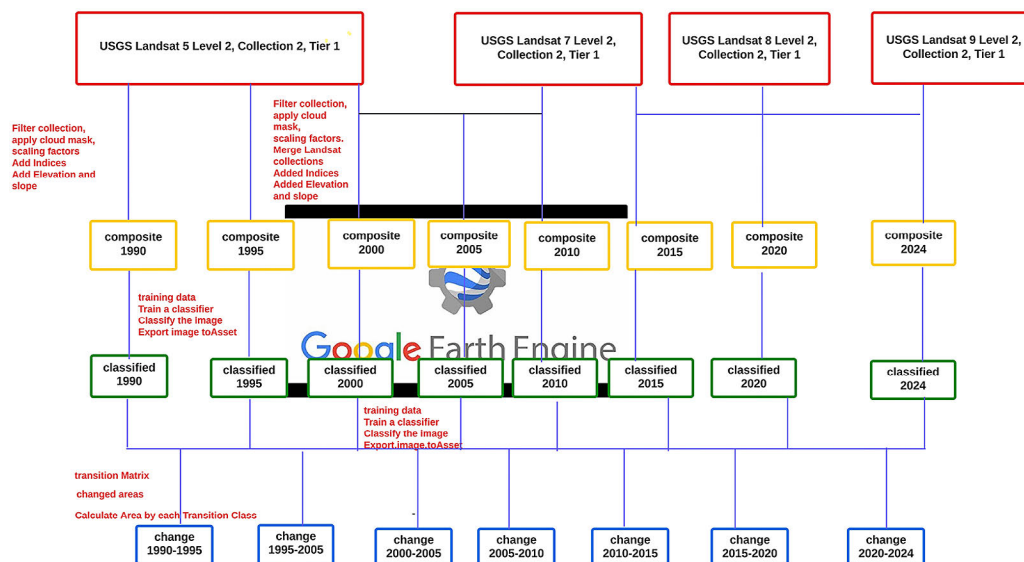


Figure 3. Flowchart methodology

Table 4. Accuracy assessment results

Year	Forest area	Confusion matrix	Test accuracy	Kappa	Producers accuracy	Consumers accuracy	Fscore
1990	43682	[[45,1],[1,42]]	0.97	0.95	[[0.97],[0.97]]	[[0.97,0.97]]	[0.97,0.97]
1995	43026	[[45,1],[2,40]]	0.96	0.93	[[0.97],[0.95]]	[[0.95,0.97]]	[0.96,0.96]
2000	38615	[[40,3],[3,34]]	0.925	0.84	[[0.93],[0.91]]	[[0.93,0.91]]	[0.93,0.91]
2005	37941	[[51,0],[1,41]]	0.98	0.97	[[1],[0.97]]	[[0.98,1]]	[0.99,0.98]
2010	36894	[[40,1],[0,41]]	0.98	0.97	[[0.97],[1]]	[[1,0.97]]	[0.98,0.98]
2015	36271	[[40,1],[6,36]]	0.91	0.83	[[0.97],[0.86]]	[[0.87,0.97]]	[0.92,0.91]
2020	35722	[[40,0],[0,35]]	1	1	[[1],[1]]	[[1],[1]]	[1,1]
2024	35522	[[46,0],[0,39]]	1	1	[[1],[1]]	[[1],[1]]	[1,1]

will allow us to follow the dynamic of the forest cover (green color). The table presents the area of the forest cover for the period 1990 to 2024 with an interval of 5 years (Figure 4).

The results show a regression of this cover over time going from 43682 ha in 1990 to 35522 ha in 2024, i.e. a regression of 8160 ha constituting a rate of 18% of the capital and a rate of 240 ha/year. This trend reflects the continued degradation of forests due to anthropogenic pressures amplified by climate change.

Accuracy assessment

As mentioned earlier in the method section, the accuracy assessment was performed by script in GEE to evaluate the accuracy of the generated maps. The accuracy results show a high agreement with the reference data. Classification accuracy remains consistently above 91%, with a peak at 100% in 2020 and 2024. This indicates

robust classification performance, validating the reliability of the methods used. The kappa statistic, which measures agreement beyond chance, demonstrates strong agreement (values ≥ 0.83) across all years. The highest values (1.0) were observed in 2020 and 2024, further confirming the reliability of the classification models. The confusion matrices indicate precise classification with minimal misclassifications. For example: In 1990, the matrix $[[45,1],[1,42]]$ shows just 2 misclassifications. By 2020 and 2024, the matrices $[[40,0],[0,35]]$ and $[[46,0],[0,39]]$ reflect perfect classification, with no misclassified samples. As for the producer’s accuracy and Consumer’s accuracy, both measures remain consistently high over the years, often exceeding 0.86, highlighting the model’s ability to accurately identify forested areas (producer’s accuracy) and correctly classify samples as forested (consumer’s accuracy). Finally, the F-score, which represents the balance between precision and recall, is also

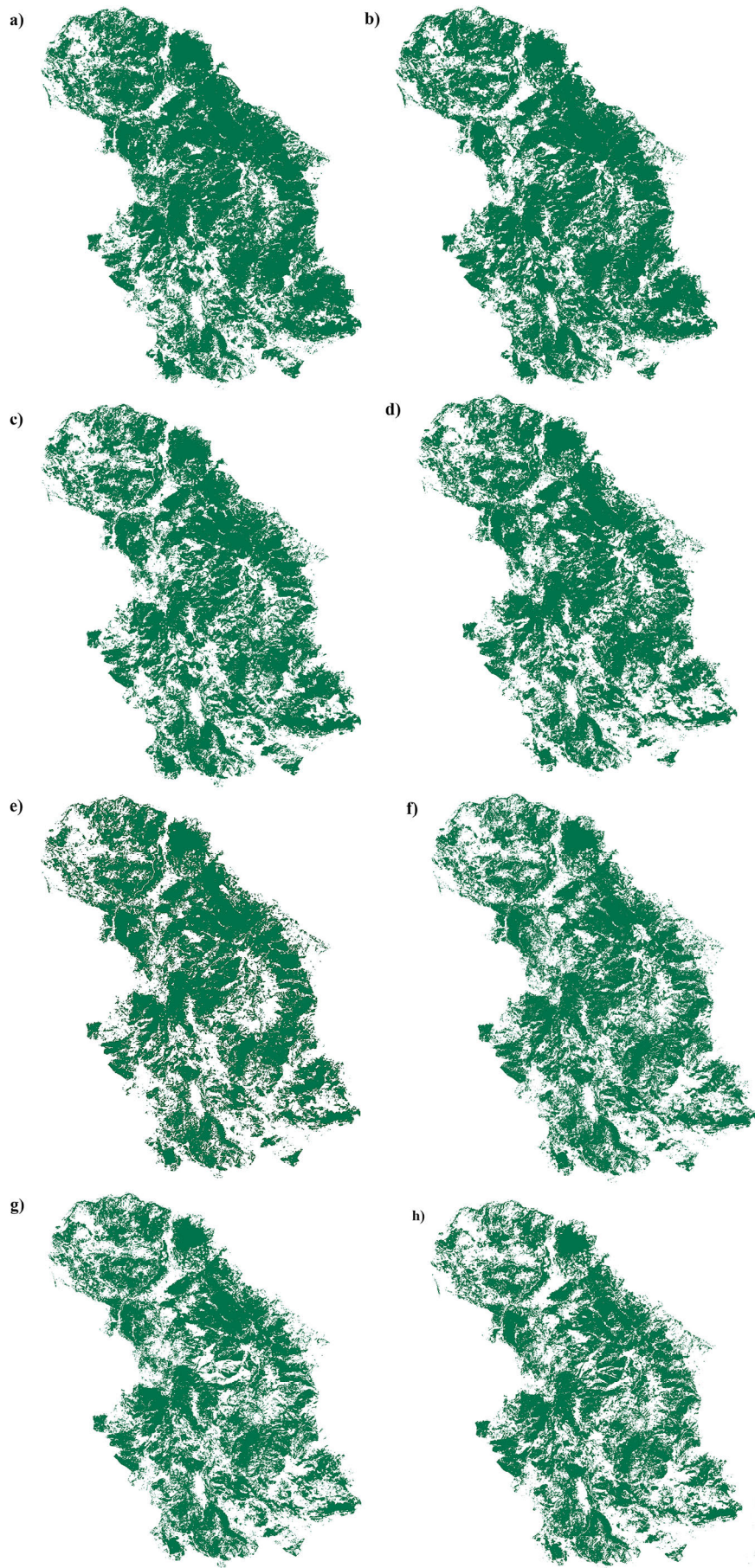


Figure 4. Classification result: (a) 1990, (b) 1995, (c) 2000, (d) 2005, (e) 2010, (f) 2015, (g)2020, (h) 2024

high (≥ 0.91) throughout the period. Perfect F-scores (1.0) in 2020 and 2024 further validate the effectiveness of the classification.

Feature importance

This analysis identifies the input features that contribute the most to the classification process, helping to refine the model by removing redundant or less impactful features. The script

serves as a powerful tool for assessing the effectiveness of individual features in a random forest model, ensuring that key predictors are appropriately prioritized (Figure 5).

Hyperparameter tuning

In this study, we used a script written in the Google Earth Engine (GEE) JavaScript API that allows hyperparameter tuning for the number of

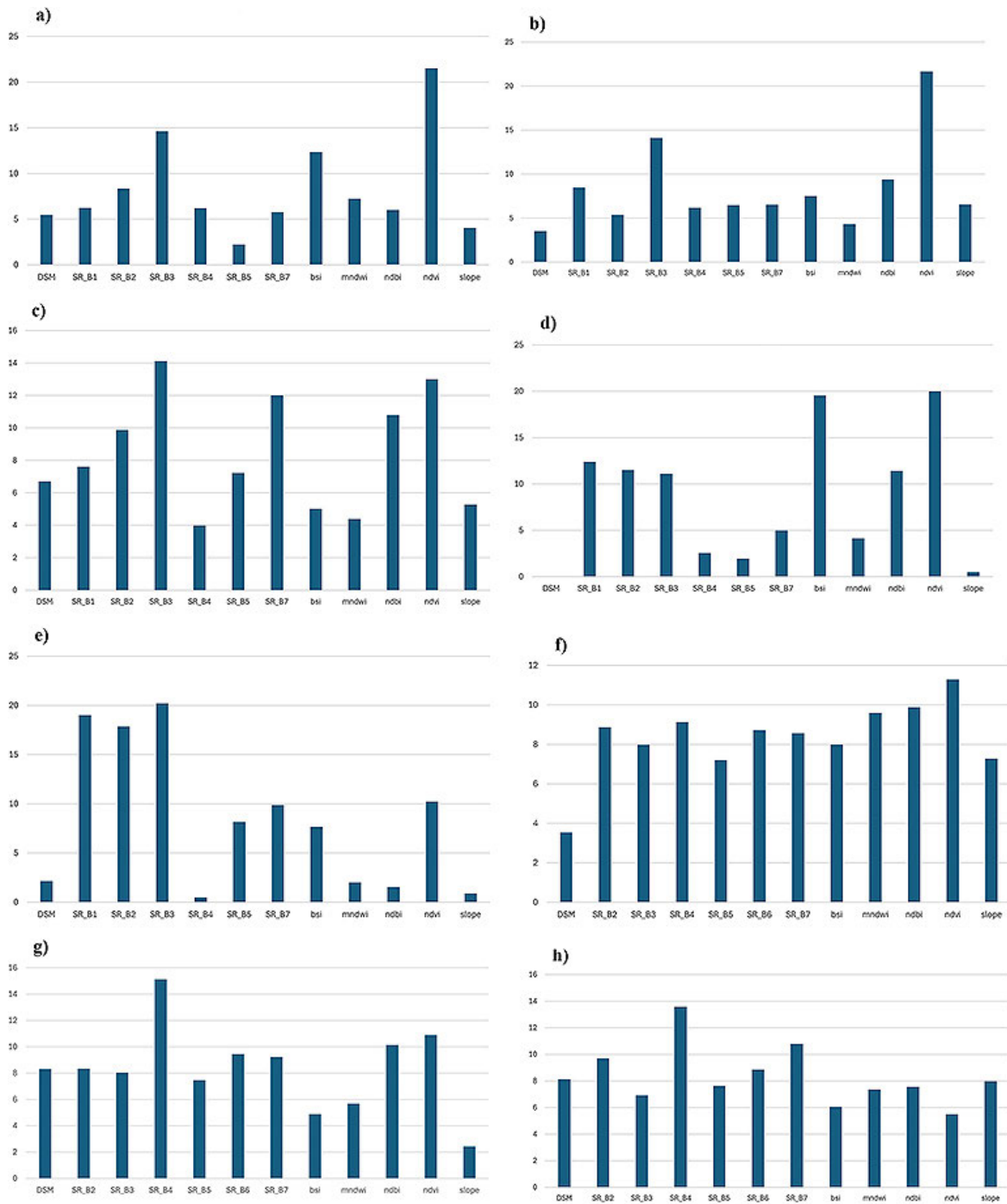


Figure 5. Feature importance: (a) 1990, (b) 1995, (c) 2000, (d) 2005, (e) 2010, (f) 2015, (g)2020, (h) 2024

trees in a random forest classifier. It consists of creating a list of numbers from 10 to 150 (inclusive), incremented by 10. Each number represents a different number of trees to test. The script generates a graph with the x-axis representing the number of trees in the random forest (numTreeList) and the y-axis representing the corresponding validation accuracy. This graph is used to identify the optimal number of trees to maximize validation accuracy (Figure 6).

Change detection analysis

Change detection analysis was performed using the categorical change method through a Java script in GEE. This analysis identifies the type of change that has occurred between two land cover maps (Figure 7). Moreover, the study provides more detail about the change by producing a transition matrix (Figure 8). The largest reduction occurred between 1995 and 2000, with a significant

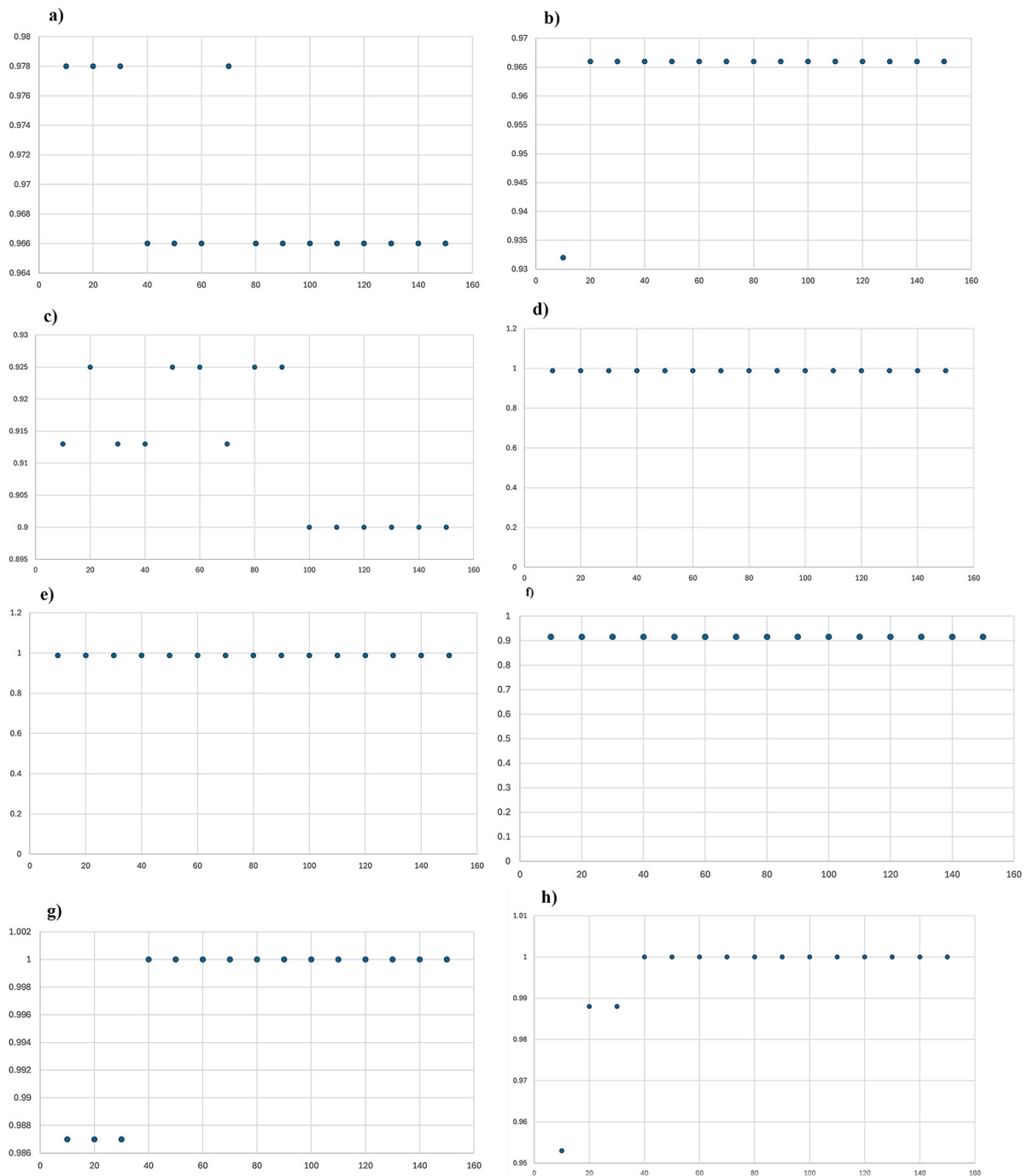


Figure 6. Hyperparameter tuning: (a) 1990, (b) 1995, (c) 2000, (d) 2005, (e) 2010, (f) 2015, (g) 2020, (h) 2024

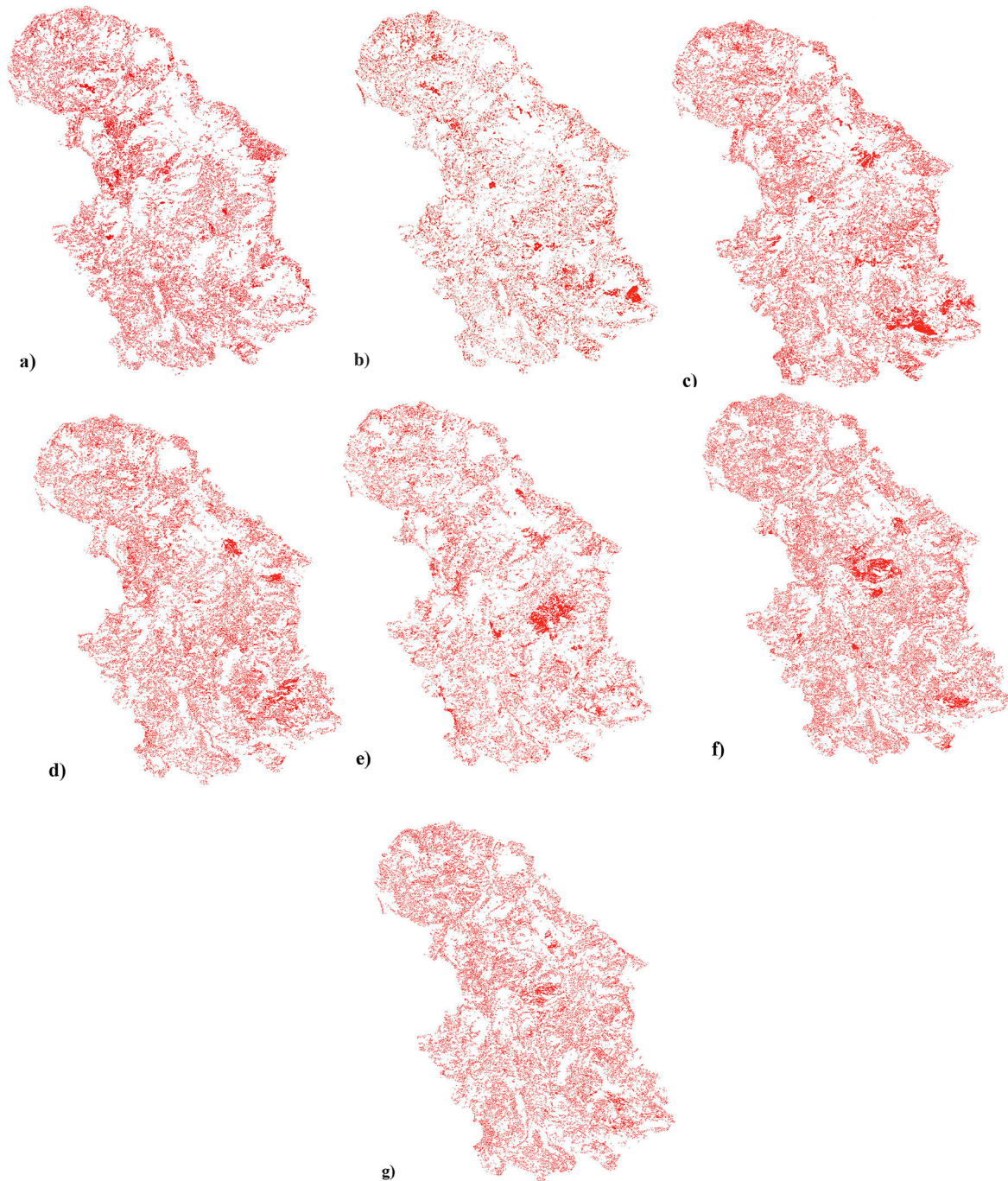


Figure 7. Change detection analysis result: (a) 1990–1995, (b) 1995–2000, (c) 2000–2005, (d) 2005–2010, (e) 2010–2015, (f), 2015–2020, (g) 2020–2024

loss of 4,411 hectares. However, the rate of decline appears to have stabilized after 2010, suggesting possible improvements in conservation efforts or a reduction in external pressures.

DISCUSSION

The TNP is renowned as a biodiversity reserve but remains vulnerable to deforestation. It

faces significant environmental challenges, including a high deforestation rate (Boubekraoui et al., 2024; Boubekroui et al., 2024). This study employed supervised classification and change detection techniques on the GEE platform, utilizing a merged composite cloud-masked image to produce LULC maps and detect temporal changes. The results revealed a substantial loss of tree cover within the TNP, which was quantified, mapped, and analyzed spatially and temporally.

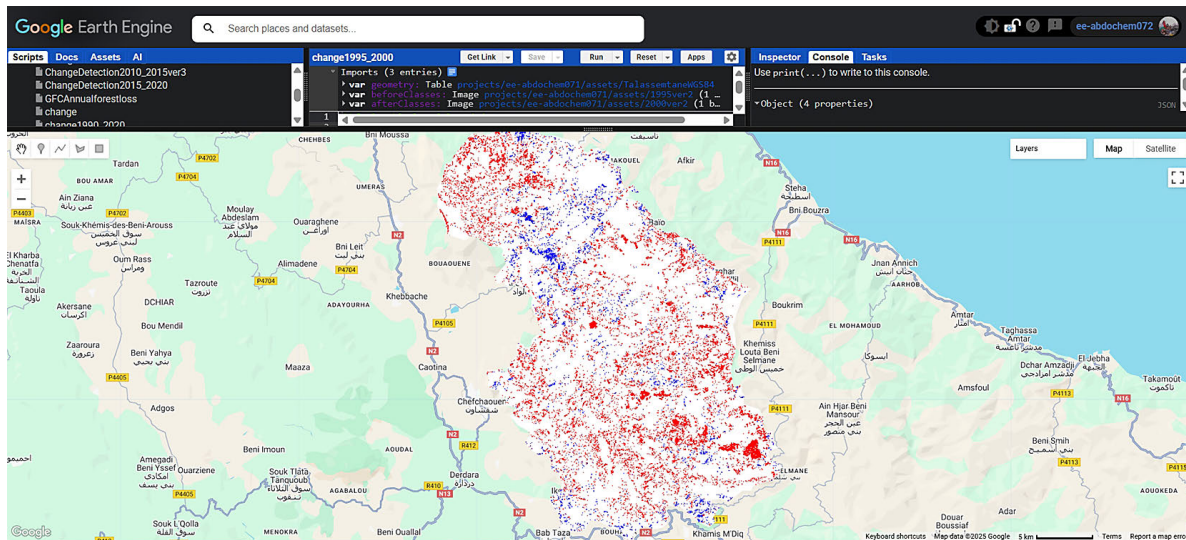


Figure 8. Distinguish between tree cover loss (red) and gain (blue)

In 1990, TNP's tree cover was estimated at 43,682 ha, representing 70% of the park's area. By 2024, this had decreased by 8.160 ha, corresponding to a 18% loss, with the most significant reduction occurring between 1995 and 2000. These findings align with other studies and reflect broader regional and global trends in forest degradation. While several studies have assessed Moroccan forest degradation trends, few have quantified this regression. Castro et al. (2022), using global forest change data, estimated an average annual loss of 106 ha within the park, ranging from 6 to 300 ha/year, with wildfires accounting for 49% of this loss (Castro et al., 2022). Another study reported an 8.39% gross loss of Western Rif forest cover (equivalent to 272.37 km²) between 2001 and 2020, identifying TNP as one of 26 deforestation fronts in the region (Boubekraoui et al., 2023). Furthermore, the Tangier-Tetouan-Al Hoceima (TTA) region recorded an average of 39.78 km²/year of burned areas, with forests comprising 74% of these losses (Boubekraoui et al., 2023). These studies also examined the primary drivers of deforestation in the region. Boubekraoui et al. (2024) identified four primary drivers of deforestation in the TTA region between 2001 and 2020: wildfires (35.2%), agricultural expansion (30.6%), logging (13.2%), and infrastructure development (10.1%) (Boubekraoui et al., 2024). Particularly in TNP, the main drivers of this degradation are forest fires combined with land clearing by local populations seeking to expand their cannabis cultivation areas (Ben-Said et al., 2020; Castro et al., 2022; Chergui et al.,

2018; Gatchui et al., 2014). Moroccan authorities, Non-Governmental Organizations and local forces are urgently called upon to intervene to stop this hemorrhage and to prohibit any practice incompatible with the environment and likely to lead to the disappearance of this beautiful ecosystem and to preserve its option value for future generations. Urgent action must be taken, including adopting a framework for participatory forest restoration and promoting a social participation in forest restoration (Derak et al., 2018, 2024). A key limitation of this study was the inability to differentiate between permanent land conversion and temporary forest loss, coupled with the lack of detailed identification of the primary drivers of deforestation. Finally, the adoption of an advanced approach that integrates SAR data with Landsat optical imagery offers more accurate insights into forest mapping and their spatiotemporal changes (Chen et al., 2018).

CONCLUSIONS

The loss of forest cover poses a significant threat to the survival of humanity, the environment, and the global climate, contributing substantially to global warming. Quantifying this threat scientifically at local, regional, and global scales has historically been challenging. However, advances in remote sensing technologies and the accessibility of high-resolution satellite imagery have addressed these constraints. In our study, we leveraged cloud-masking image collection

through the GEE platform to assess deforestation in the TNP between 1995 and 2024. This approach proved especially valuable given the absence of updated national data since the 2004 National Forest Inventory. By utilizing these tools, we were able to calculate the extent and loss of forest cover within the TNP, providing critical insights for forest management.

The methods and findings of this study provide a valuable resource for decision-makers and forest managers to track deforestation trends and assess the effectiveness of conservation and restoration efforts. These tools not only enhance understanding of forest ecosystem dynamics but also support evidence-based strategies for sustainable forest management. In addition, the results of this study can be utilized to predict future land use and land cover changes, providing valuable insights for sustainable forest management and conservation planning.

REFERENCES

1. Aafi, A. (2000). Floristic diversity of Morocco's fir ecosystem (*Abies maroccana* Trab.) (Talassemtane National Park). *Nature et Faune* 16(1), 20–23.
2. Abuelaish, B., & Olmedo, M. T. C. (2016). Scenario of land use and land cover change in the Gaza Strip using remote sensing and GIS models. *Arabian Journal of Geosciences*, 9(4). <https://doi.org/10.1007/s12517-015-2292-7>
3. Acharki, S., El Qorchi, F., Arjald, Y., Amharref, M., Bernoussi, A. S., & Ben Aissa, H. (2022). Soil erosion assessment in Northwestern Morocco. *Remote Sensing Applications: Society and Environment*, 25(November 2021), 100663. <https://doi.org/10.1016/j.rsase.2021.100663>
4. Ait M'Barek, S., Bouslihim, Y., Rochdi, A., Miftah, A., & Beroho, M. (2024). The combined impact of climate change scenarios and land use changes on water resources in a semi-arid watershed. *Scientific African*, 25(February), e02319. <https://doi.org/10.1016/j.sciaf.2024.e02319>
5. Ait El Haj, F., Oquadif, L., & Akhssas, A. (2023). Monitoring land use and land cover changes using remote sensing techniques and the precipitation-vegetation indexes in Morocco. *Ecological Engineering and Environmental Technology*, 24(1), 272–286. <https://doi.org/10.12912/27197050/154937>
6. Alaoui, A., Laaribya, S., Ayan, S., Ghallab, A., & López-Tirado, J. (2021). Modelling spatial distribution of endemic Moroccan fir (*Abies marocana* Trab.) in Talassemtane National Park, Morocco. *Austrian Journal of Forest Science*, 138(2), 73–93.
7. Alaoui, H. I., Chemchaoui, A., & Kacem, H. A. (2024). Economic valuation of sediment retention services in the Oued-Beht watershed (Morocco): A spatiotemporal analysis using InVEST SDR-InVEST model. *Ecological Frontiers*, May. <https://doi.org/10.1016/j.ecofro.2024.05.003>
8. Alshari, E. A., & Gawali, B. W. (2021). Development of classification system for LULC using remote sensing and GIS. *Global Transitions Proceedings*, 2(1), 8–17. <https://doi.org/10.1016/J.GLTP.2021.01.002>
9. Amani, M., Ghorbanian, A., Ahmadi, S. A., Karkoei, M., Moghimi, A., Mirmazloumi, S. M., Moghaddam, S. H. A., Mahdavi, S., Ghahremanloo, M., Parsian, S., Wu, Q., & Brisco, B. (2020). Google Earth Engine Cloud Computing Platform for Remote Sensing Big Data Applications: A Comprehensive Review. *IEEE Journal of Selected Topics in Applied Earth Observations and Remote Sensing*, 13(September), 5326–5350. <https://doi.org/10.1109/JSTARS.2020.3021052>
10. Aouragh, M. H., Ijlil, S., Essahlaoui, N., Essahlaoui, A., El Hmaidi, A., El Ouali, A., & Mridekh, A. (2023). Remote sensing and GIS-based machine learning models for spatial gully erosion prediction: A case study of Rdat watershed in Sebou basin, Morocco. *Remote Sensing Applications: Society and Environment*, 30(January), 100939. <https://doi.org/10.1016/j.rsase.2023.100939>
11. Araya, Y. H., & Cabral, P. (2010). Analysis and modeling of urban land cover change in Setúbal and Sesimbra, Portugal. *Remote Sensing*, 2(6), 1549–1563. <https://doi.org/10.3390/rs2061549>
12. Aziz, G., Minallah, N., Saeed, A., Frnda, J., & Khan, W. (2024). Remote sensing based forest cover classification using machine learning. *Scientific Reports*, 14(1), 1–17. <https://doi.org/10.1038/s41598-023-50863-1>
13. Bammou, Y., Benzougagh, B., Abdessalam, O., Brahim, I., Kader, S., Spalevic, V., Sestras, P., & Ercişli, S. (2024). Machine learning models for gully erosion susceptibility assessment in the Tensift catchment, Haouz Plain, Morocco for sustainable development. *Journal of African Earth Sciences*, 213, 105229. <https://doi.org/10.1016/J.JAFREARSCI.2024.105229>
14. Bannari, A., Morin, D., Bonn, F., & Huete, A. R. (1995). A review of vegetation indices. *Remote Sensing Reviews*, 13(1–2), 95–120. <https://doi.org/10.1080/02757259509532298>
15. Benchelha, N., Bezza, M., Belbounaguia, N., Benchelha, S., & Benchelha, M. (2022). Modeling Dynamic Urban Growth Using Cellular Automata and Geospatial Technique: Case of Casablanca in Morocco. *International Journal of Geoinformatics*, 18(5), 27–40. <https://doi.org/10.52939/ijg.v18i5.2369>

16. Ben-Said, M. (2022). The taxonomy of Moroccan fir *Abies marocana* (Pinaceae): conceptual clarifications from phylogenetic studies. *Mediterranean Botany*, 43(April). <https://doi.org/10.5209/mbot.71201>
17. Ben-said, M., Chemchaoui, A., Etebaai, I. et al. Land use and land cover changes in Morocco: trends, research gaps, and perspectives. *Geo-Journal* 90, 44 (2025). <https://doi.org/10.1007/s10708-024-11214-3>
18. Ben-said, M., Berrad, F., & Abdelilah, G. (2024). *Etat des connaissances sur la sapinière endémique du Maroc (Abies marocana Trab.): acquis, lacunes et nouveaux axes de recherche. Bulletin de l'Institut Scientifique, Rabat, Section Sciences de la Vie n° 46(May), 01–16 (2024).*
19. Ben-Said, M., Ghallab, A., Lamrhari, H., Carreira, J. A., Linares, J. C., & Taïqui, L. (2020). Characterizing spatial structure of *Abies marocana* forest through point pattern analysis. *Forest Systems*, 29(2), 1–13. <https://doi.org/10.5424/fs/2020292-16754>
20. Ben-Said, M., Linares, J. C., Antonio Carreira, J., & Taïqui, L. (2022). Spatial patterns and species coexistence in mixed *Abies marocana-Cedrus atlantica* forest in Talassemtane National Park. *Forest Ecology and Management*, 506(October 2021). <https://doi.org/10.1016/j.foreco.2021.119967>
21. Benzyane, M. (2007). La gestion durable des ressources forestières au Maroc: quelle stratégie ? *Forêt Méditerranéenne*, T. XXVIII(1), 47–54. <https://hal.archives-ouvertes.fr/hal-03565302/document>
22. Boubekraoui, H., Attar, Z., Maouni, Y., Ghallab, A., Saidi, R., & Maouni, A. (2024). Forest loss drivers and landscape pressures in a Northern Moroccan protected areas' network: Introducing a novel approach for conservation effectiveness assessment. In *Conservation* 4(3). <https://doi.org/10.3390/conservation4030029>
23. Boubekraoui, H., Maouni, Y., Ghallab, A., & Draoui, M. (2023). Trees, Forests and People Spatio-temporal analysis and identification of deforestation hotspots in the Moroccan western Rif. *Trees, Forests and People*, 12(December 2022), 100388. <https://doi.org/10.1016/j.tfp.2023.100388>
24. Boubekraoui, H., Maouni, Y., Ghallab, A., & Draoui, M. (2024). *Deforestation drivers in northern Morocco : an exploratory spatial data analysis.* Environmental Research Communications 6 (2024) 071005. <https://doi.org/10.1088/2515-7620/ad5ad6>
25. Boubekraoui, H., Maouni, Y., Ghallab, A., Draoui, M., & Maouni, A. (2023). Wildfires risk assessment using hotspot analysis and results application to wildfires strategic response in the Region of Tangier-Tetouan-Al Hoceima, Morocco. *Fire*, 6(8). <https://doi.org/10.3390/fire6080314>
26. Castro, I., Stan, A. B., Taiqui, L., Schiefer, E., Ghallab, A., Derak, M., & Fulé, P. Z. (2022). Detecting fire-caused forest loss in a Moroccan protected area. *Fire*, 5(2). <https://doi.org/10.3390/fire5020051>
27. Chang, Y., Hou, K., Li, X., Zhang, Y., & Chen, P. (2018). Review of Land Use and Land Cover Change research progress. *IOP Conference Series: Earth and Environmental Science*, 113(1). <https://doi.org/10.1088/1755-1315/113/1/012087>
28. Chebli, Y., Chentouf, M., Ozer, P., Hornick, J. L., & Cabaraux, J. F. (2018). Forest and silvopastoral cover changes and its drivers in northern Morocco. *Applied Geography*, 101(November), 23–35. <https://doi.org/10.1016/j.apgeog.2018.10.006>
29. Chen, B., Xiao, X., Ye, H., Ma, J., Doughty, R., Li, X., & Zhao, B. (2018). *Mapping Forest and Their Spatial – Temporal Changes From 2007 to 2015 in Tropical Hainan Island by Integrating ALOS / ALOS-2 L-Band SAR and Landsat Optical Images.* 11(3), 852–867.
30. Chergui, B., Fahd, S., Santos, X., & Pausas, J. G. (2018). Socioeconomic factors drive fire-regime variability in the Mediterranean Basin. *Ecosystems*, 21(4), 619–628. <https://doi.org/10.1007/s10021-017-0172-6>
31. Congalton, R. G., & Green, K. (2008). *Assessing The Accuracy of Remotely Sensed Data :Principles and Practices.* CRC Press; 2nd edition (December 12, 2008).
32. Curtis, P. G., Slay, C. M., Harris, N. L., Tyukavina, A., & Hansen, M. C. (2018). Classifying drivers of global forest loss. *Science*, 361(6407), 1108–1111. <https://doi.org/10.1126/science.aau3445>
33. Département des Eaux et Forêts Maroc. (2019). *Présentation de la nouvelle stratégie Forêts du Maroc.* <https://www.youtube.com/watch?v=8laKNHBYfDE>
34. Derak, M., Cortina, J., Taiqui, L., & Aledo, A. (2018). A proposed framework for participatory forest restoration in semiarid areas of North Africa. *Restoration Ecology*, 26, 18–25. <https://doi.org/10.1111/rec.12486>
35. Derak, M., Taiqui, L., Fiedler, S., & Cortina-Segarra, J. (2024). Social learning to promote forest restoration in a semi-arid landscape in North Africa. *Environmental Development*, 49(February), 100972. <https://doi.org/10.1016/j.envdev.2024.100972>
36. Eshetie, A. A., Wubneh, M. A., Kiflew, M. S., & Alemu, M. G. (2023). Application of artificial neural network (ANN) for investigation of the impact of past and future land use – land cover change on streamflow in the Upper Gilgel Abay watershed, Abay Basin, *Applied Water Science.* <https://doi.org/10.1007/s13201-023-02003-3>
37. Es-smairi, A., Elmoutchou, B., Mir, R. A., Ouazani Touhami, A. El, & Namous, M. (2023). Delineation of landslide susceptible zones using Frequency

- Ratio (FR) and Shannon Entropy (SE) models in northern Rif, Morocco. *Geosystems and Geoenvironment*, 2(4), 100195. <https://doi.org/10.1016/j.geogeo.2023.100195>
38. FAO. (2022). *Forest Ressources Assessment 2020 Remote Sensing Survey* (FAO, Ed.; FORESTRY P). FAO. <https://doi.org/10.4060/cb9970en>
39. Farah, A., Algouti, A., Algouti, A., Adaze, E., & Ifkirne, M. (2021). Remote sensing for land use mapping, case of the study area: Urban commune of Saada, Morocco. *Journal of Environmental and Agricultural Studies*, 2(1), 36–43. <https://doi.org/10.32996/jeas.2021.2.1.3>
40. Foody, G. M. (2010). Assessing the accuracy of land cover change with imperfect ground reference data. *Remote Sensing of Environment*, 114(10), 2271–2285. <https://doi.org/10.1016/j.rse.2010.05.003>
41. García-álvarez, D., Teresa, M., & Olmedo, C. (2022). Land use cover datasets and validation tools. In *Land Use Cover Datasets and Validation Tools*. <https://doi.org/10.1007/978-3-030-90998-7>
42. Gatchui, H. C., Smektala, G., Solano, D., Taiqui, L., & Ngomeni, A. F. (2014). *Cannabis cultivation and deforestation in the Site of Bio Ecological Interest (SIBE) of Bouhachem, Morocco*. 8(June), 1179–1191.
43. Ghazi, S., Ziri, R., Brhadda, N., Chemchaoui, A., Alaoui, H. I., Boukita, H., Asri, B. El, & Jdi, L. (2024). Cork oak in the Maamora Forest (Morocco) – Updating its distribution and optimizing cork productivity for sustainable development. *Ecological Engineering and Environmental Technology*, 25(1), 288–299. <https://doi.org/10.12912/27197050/175651>
44. Ghosh, S., Kumar, D., & Kumari, R. (2022). Cloud-based large-scale data retrieval, mapping, and analysis for land monitoring applications with Google Earth Engine (GEE). *Environmental Challenges*, 9(November 2021), 100605. <https://doi.org/10.1016/j.envc.2022.100605>
45. Gorelick, N., Hancher, M., Dixon, M., Ilyushchenko, S., Thau, D., & Moore, R. (2017). Google Earth Engine: Planetary-scale geospatial analysis for everyone. *Remote Sensing of Environment*, 202, 18–27. <https://doi.org/10.1016/j.rse.2017.06.031>
46. Hansen, M. C., Potapov, P. V., Moore, R., Hancher, M., Turubanova, S. A., Tyukavina, A., Thau, D., Stehman, S. V., Goetz, S. J., Loveland, T. R., Kommareddy, A., Egorov, A., Chini, L., Justice, C. O., & Townshend, J. R. G. (2013). High-resolution global maps of 21st-century forest cover change. *Science*, 342(6160), 850–853. <https://doi.org/10.1126/science.1244693>
47. Haut-Commissariat au Plan du Maroc. (2024). *Recensement General de la Population et l'Habitat de 2024*. https://resultats2024.rgphapps.ma/superset/dashboard/0fbd169b-19e1-4338-a344-e58b-b9a02a4d/?permalink_key=pmo6qLqylzY&standalone=true
48. He, Y., Chipman, J., Siegert, N., & Mankin, J. S. (2022). Rapid land-cover and land-use change in the Indo-Malaysian Region over the last thirty-four years based on AVHRR NDVI data. *Annals of the American Association of Geographers*, 0(0), 1–21. <https://doi.org/10.1080/24694452.2022.2077168>
49. Hegazy, I. R., & Kaloop, M. R. (2015). Monitoring urban growth and land use change detection with GIS and remote sensing techniques in Daqahlia governorate Egypt. *International Journal of Sustainable Built Environment*, 4(1), 117–124. <https://doi.org/10.1016/J.IJSBE.2015.02.005>
50. Hermosilla, T., Francini, S., Nicolau, A. P., Wulder, M. A., White, J. C., Coops, N. C., & Chirici, G. (2024). Cloud-Based Remote Sensing with Google Earth Engine. In *Cloud-Based Remote Sensing with Google Earth Engine* (Issue October). Springer International Publishing. <https://doi.org/10.1007/978-3-031-26588-4>
51. Ismaili Alaoui, H., Chemchaoui, A., El Asri, B., Ghazi, S., Brhadda, N., & Ziri, R. (2023). Modeling predictive changes of carbon storage using invest model in the Beht watershed (Morocco). *Modeling Earth Systems and Environment*, 0123456789. <https://doi.org/10.1007/s40808-023-01697-3>
52. Janssen, L. L. F., & van der Wel, F. J. M. (1994). Accuracy assessment of satellite derived land-cover data: A review. *Photogrammetric Engineering and Remote Sensing*, 60(4), 419–426.
53. Jia, N., Jiyuan, L. I. U., Wenhui, K., Xinliang, X. U., & Shuwen, Z. (2018). *Spatiotemporal patterns and characteristics of land-use change in China during 2010 – 2015*. 28(2017), 547–562.
54. Kaur, H., Tyagi, S., Mehta, M., & Singh, D. (2023). Time series (2001/2002–2021) analysis of Earth observation data using Google Earth Engine (GEE) for detecting changes in land use land cover (LULC) with specific reference to forest cover in East Godavari Region, Andhra Pradesh, India. *Journal of Earth System Science*, 132(2). <https://doi.org/10.1007/s12040-023-02099-w>
55. Fikri-Benbrahim, K., Ismaili, M., Fikri Benbrahim, S., & Tribak, A. (2004). Problems of environmental degradation by desertification and deforestation: the impact of the phenomenon in Morocco. *Sécheresse*, 15(4), 307–320.
56. l'Agence Nationale des Eaux et Forêts Maroc. (2025). *Forêts En Chiffres*. <http://www.eauxetforets.gov.ma>
57. Lamrhari, H., Ben-Said, M., Jalal, Z., El Mehraz, D., & Bouziane, H. (2020). Morphological and Anatomical Characteristics of Moroccan Fir Needles in Talassemthane National Park, North-Western Rif Region, Morocco. *European Scientific Journal ESJ*, 16(33), 189–205. <https://doi.org/10.19044/esj.2020.v16n33p189>

58. Lawer, E. A. (2024). An evaluation of single and multi-date Landsat image classifications using random forest algorithm in a semi-arid savanna of Ghana, West Africa. *Scientific African*, 26, e02434. <https://doi.org/10.1016/j.sciaf.2024.e02434>
59. Lin, L., Hao, Z., Post, C. J., Mikhailova, E. A., Yu, K., Yang, L., & Liu, J. (2020). Monitoring land cover change on a rapidly urbanizing island using google earth engine. *Applied Sciences (Switzerland)*, 10(20), 1–16. <https://doi.org/10.3390/app10207336>
60. Lloyd, D. (1990). A phenological classification of terrestrial vegetation cover using shortwave vegetation index imagery. *International Journal of Remote Sensing*, 11(12), 2269–2279. <https://doi.org/10.1080/01431169008955174>
61. Lu, D., Mausel, P., Brondízio, E., & Moran, E. (2004). Change detection techniques. *International Journal of Remote Sensing*, 25(12), 2365–2401. <https://doi.org/10.1080/0143116031000139863>
62. Moumane, A., Al Karkouri, J., Benmansour, A., El Ghazali, F. E., Fico, J., Karmaoui, A., & Batchi, M. (2022). Monitoring long-term land use, land cover change, and desertification in the Ternata oasis, Middle Draa Valley, Morocco. *Remote Sensing Applications: Society and Environment*, 26(April), 100745. <https://doi.org/10.1016/j.rsase.2022.100745>
63. Muhammad, R., Zhang, W., Abbas, Z., Guo, F., & Gwiazdzinski, L. (2022). Spatiotemporal change analysis and prediction of future land use and land cover changes using QGIS MOLUSCE plugin and remote sensing big data: A case study of Linyi, China. *Land*, 11(3). <https://doi.org/10.3390/land11030419>
64. Muteya, K., Nghonda, D. N. T., Kalenda, F. M., Strammer, H., Kankumbi, F. M., Malaisse, F., Bastin, J., Sikuzani, Y. U., & Bogaert, J. (2023). *Mapping and Quantification of Miombo Deforestation in the Extent and Changes between 1990 and 2022*.
65. Nguyen, T. T., Aderdour, N., Rhinane, H., & Buerkert, A. (2023). Vegetation cover dynamics in the high atlas mountains of Morocco. *Remote Sensing*, 15(5). <https://doi.org/10.3390/rs15051366>
66. Oldeland, J., Dorigo, W., Lieckfeld, L., Lucieer, A., & Jürgens, N. (2010). Combining vegetation indices, constrained ordination and fuzzy classification for mapping semi-natural vegetation units from hyperspectral imagery. *Remote Sensing of Environment*, 114(6), 1155–1166. <https://doi.org/10.1016/j.rse.2010.01.003>
67. Ouchra, H., Belangour, A., & Erraissi, A. (2023). Machine Learning Algorithms for Satellite Image Classification Using Google Earth Engine and Landsat Satellite Data: Morocco Case Study. *IEEE Access*, 11(July), 71127–71142. <https://doi.org/10.1109/ACCESS.2023.3293828>
68. Ouchra, H., Belangour, A., & Erraissi, A. (2024). Supervised Machine Learning Algorithms for Land Cover Classification in Casablanca, Morocco. *Ingenierie Des Systemes d'Information*, 29(1), 377–387. <https://doi.org/10.18280/isi.290137>
69. Pérez-cutillas, P., Pérez-navarro, A., Conesa-garcía, C., Zema, D. A., & Amado-álvarez, J. P. (2023). Remote Sensing Applications : Society and Environment What is going on within google earth engine ? A systematic review and meta-analysis. *Remote Sensing Applications: Society and Environment*, 29(December 2022), 100907. <https://doi.org/10.1016/j.rsase.2022.100907>
70. Rachid, L., Elmostafa, A., Mehdi, M., & Hassan, R. (2024). Assessing carbon storage and sequestration benefits of urban greening in Nador City, Morocco, utilizing GIS and the InVEST model. *Sustainable Futures*, 7(November 2023), 100171. <https://doi.org/10.1016/j.sfr.2024.100171>
71. Raqeeb, A., Saleem, A., Ansari, L., Nazami, S. M., Muhammad, M. W., Malik, M., Naqash, M., & Khalid, F. (2024). Assessment of land use cover changes, carbon sequestration and carbon stock in dry temperate forests of Chilas watershed, Gilgit-Baltistan. *Brazilian Journal of Biology*, 84, 1–16. <https://doi.org/10.1590/1519-6984.253821>
72. Seyam, M. M. H., Haque, M. R., & Rahman, M. M. (2023). Identifying the land use land cover (LULC) changes using remote sensing and GIS approach: A case study at Bhaluka in Mymensingh, Bangladesh. *Case Studies in Chemical and Environmental Engineering*, 7(November 2022), 100293. <https://doi.org/10.1016/j.cscee.2022.100293>
73. Tadono, T., Ishida, H., Oda, F., Naito, S., Minakawa, K., & Iwamoto, H. (2014). Precise Global DEM Generation by ALOS PRISM. *ISPRS Annals of the Photogrammetry, Remote Sensing and Spatial Information Sciences*, II-4(May), 71–76. <https://doi.org/10.5194/isprsannals-ii-4-71-2014>
74. Talukdar, S., Singha, P., Mahato, S., Shahfahad, Pal, S., Liou, Y. A., & Rahman, A. (2020). Land-use land-cover classification by machine learning classifiers for satellite observations-A review. In *Remote Sensing* 12(7). MDPI AG. <https://doi.org/10.3390/rs12071135>
75. Tamiminia, H., Salehi, B., Mahdianpari, M., Quackenbush, L., Adeli, S., & Brisco, B. (2020). Google Earth Engine for geo-big data applications: A meta-analysis and systematic review. *ISPRS Journal of Photogrammetry and Remote Sensing*, 164(January), 152–170. <https://doi.org/10.1016/j.isprsjprs.2020.04.001>
76. Ustuner, M., Sanli, F. B., Abdikan, S., Esetlili, M. T., & Kurucu, Y. (2014). Crop type classification using vegetation indices of rapideye imagery. *International Archives of the Photogrammetry, Remote Sensing and Spatial Information Sciences - ISPRS*

- Archives*, 40(7), 195–198. <https://doi.org/10.5194/isprsarchives-XL-7-195-2014>
77. Vinayak, B., Lee, H. S., & Gedem, S. (2021). Prediction of land use and land cover changes in Mumbai city, India, using remote sensing data and a multilayer perceptron neural network-based Markov Chain model. *Sustainability (Switzerland)*, 13(2), 1–22. <https://doi.org/10.3390/su13020471>
78. Wang, H., Liu, C., Zang, F., Yang, J., Li, N., Rong, Z., & Zhao, C. (2020). Impacts of topography on the land cover classification in the Qilian Mountains, Northwest China. *Canadian Journal of Remote Sensing*, 46(3), 344–359. <https://doi.org/10.1080/07038992.2020.1801401>
79. Wang, S., He, S., Wang, J., Li, J., Zhong, X., Cole, J., Kurbanov, E., & Sha, J. (2023). Analysis of land use/cover changes and driving forces in a typical subtropical region of South Africa. *Remote Sensing*, 15(19), 1–19. <https://doi.org/10.3390/rs15194823>
80. Wang, S. W., Munkhnasan, L., & Lee, W. K. (2021). Land use and land cover change detection and prediction in Bhutan's high altitude city of Thimphu, using cellular automata and Markov chain. *Environmental Challenges*, 2(November 2020). <https://doi.org/10.1016/j.envc.2020.100017>
81. Weng, Q., Li, Z., Cao, Y., Lu, X., Gamba, P., Zhu, X., Xu, Y., Zhang, F., Qin, R., Yang, M. Y., Ma, P., Huang, W., Yin, T., Zheng, Q., Zhou, Y., & Asner, G. (2024). How will ai transform urban observing, sensing, imaging, and mapping? *Npj Urban Sustainability*, 4(1). <https://doi.org/10.1038/s42949-024-00188-3>
82. Wulder, M. A., Franklin, S. E., White, J. C., Cranny, M. M., & Dechka, J. A. (2004). Inclusion of topographic variables in an unsupervised classification of satellite imagery. *Canadian Journal of Remote Sensing*, 30(2), 137–149. <https://doi.org/10.5589/m03-063>
83. Yangouliba, G. I., Zoungrana, B. J. B., Hackman, K. O., Koch, H., Liersch, S., Sintondji, L. O., Dipama, J. M., Kwawuvi, D., Ouedraogo, V., Yabr e, S., Bonkougou, B., Sougu e, M., Gadiaga, A., & Koffi, B. (2022). Modelling past and future land use and land cover dynamics in the Nakambe River Basin, West Africa. *Modeling Earth Systems and Environment*, 0123456789. <https://doi.org/10.1007/s40808-022-01569-2>
84. Zeng, Z., Estes, L., Ziegler, A. D., Chen, A., Searchinger, T., Hua, F., Guan, K., Jintrawet, A., & F. Wood, E. (2018). Highland cropland expansion and forest loss in Southeast Asia in the twenty-first century. *Nature Geoscience*, 11(8), 556–562. <https://doi.org/10.1038/s41561-018-0166-9>
85. Zhang, Y., Yang, W., Sun, Y., Chang, C., Yu, J., & Zhang, W. (2021). Fusion of multispectral aerial imagery and vegetation indices for machine learning-based ground classification. *Remote Sensing*, 13(8). <https://doi.org/10.3390/rs13081411>
86. Zhao, Y., Zhang, K., Fu, Y., & Zhang, H. (2012). Examining land-use/land-cover change in the lake dianchi watershed of the Yunnan-Guizhou plateau of Southwest China with remote sensing and GIS techniques: 1974-2008. *International Journal of Environmental Research and Public Health*, 9(11), 3843–3865. <https://doi.org/10.3390/ijerph9113843>